Acta Pharmacologica Sinica (2013) 34: 1420–1426
 1671-4083/13 $32.00
www.nature.com/aps

Original Article

Effects of ketoconazole and rifampicin on the pharmacokinetics of GLS4, a novel anti-hepatitis B virus compound, in dogs

Xin ZHOU, Zhi-wei GAO, Jian MENG, Xiao-yan CHEN, Da-fang ZHONG*

Centre for Drug Metabolism and Pharmacokinetics Research, Shanghai Institute of Materia Medica, Chinese Academy of Sciences, Shanghai 201203, China

Aim: To investigate the metabolism of GLS4, a heteroaryldihydropyrimidine compound with anti-hepatitis B virus activity, in dog and human liver microsomes *in vitro* and evaluate the effects of ketoconazole (a potent CYP3A inhibitor) or rifampicin (a potent CYP3A inducer) on GLS4 pharmacokinetics in dogs.
Methods: Dog and human liver microsomes and CYP3A4 were incubated with [^{14}C]GLS4 for 15 min and then analyzed using a HPLC-dynamic online radio flow detection method. Two groups of beagle dogs were used for *in vivo* studies. Group A were orally administered a single dose of GLS4 (15 mg/kg) with or without ketoconazole pretreatment (100 mg/d for 8 consecutive days). Group B were orally administered a single dose of GLS4 (15 mg/kg) with or without rifampicin pretreatment (100 mg/d for 8 consecutive days). Plasma was sampled after GLS4 dosing. GLS4 concentrations were determined by HPLC-tandem mass spectrometry.
Results: The metabolic profile of [^{14}C]GLS4 in human and dog liver microsomes and CYP3A4 was similar. The major metabolites were morpholine *N*-dealkylated GLS4 and morpholine *N*,*N*-di-dealkylated GLS4. Pretreatment with ketoconazole or rifampicin significantly affected the plasma concentrations of GLS4 in dogs: ketoconazole increased the area under the concentration-time curve from 0 to infinity and peak concentration of GLS4 by 4.4 and 3.3 folds, respectively, whereas rifampicin decreased these parameters by 88.5% and 83.2%, respectively.
Conclusion: GLS4 is a sensitive substrate of CYP3A. CYP3A inhibitors or inducers cause considerable change of GLS4 plasma concentrations in dogs, which should be considered in clinical practice.

Keywords: GLS4; ketoconazole; rifampicin; CYP3A; drug–drug interaction; hepatitis B virus

Acta Pharmacologica Sinica (2013) 34: 1420–1426; doi: 10.1038/aps.2013.76; published online 23 Sep 2013

Introduction

Hepatitis B virus (HBV) infection is a major global health problem, and approximately 5% of the world population is infected with HBV[1]. The virus is endemic in China and other parts of Asia. Up to 10% of the population in these areas are affected by chronic HBV infection[2].

Agents approved for the treatment of HBV include interferon and nucleoside analogues[3]. However, these drugs do not have sufficient effects and may exhibit some unexpected side effects[4–6]. Compared with interferon and nucleoside analogues, heteroaryldihydropyrimidines such as Bay41-4109 and Bay39-5493 are a new series of anti-HBV compounds and reported to inhibit HBV replication by drug-induced depletion of nucleocapsids[7].

* To whom correspondence should be addressed.
E-mail dfzhong@mail.shcnc.ac.cn
Received 2013-03-09 Accepted 2013-05-09

GLS4 (4-[2-bromo-4-fluorophenyl]-6-morpholino-methyl]-2-[2-thiazolyl]-1,4-dihydro-pyrimidine-5-carboxylate, Figure 1), a new heteroaryldihydropyrimidine compound, was developed from Bay41-4109 on the basis of drug-like properties. GLS4 is a potent inhibitor on the replication of both wild-type and adefovir-resistant HBV with IC_{50} of 12 nmol/L[8]. It targets HBV capsid formation, a process which is necessary for genome replication and is assumed to be less prone to developing drug resistance[8]. Therefore, GLS4 has potential clinical applications. GLS4 is currently under phase I clinical trials in China and displays good pharmacokinetic behaviors and tolerance.

Potential drug–drug interactions between an investigational new drug and other drugs should be defined during drug development as part of an adequate assessment of the safety and effectiveness of the drug[9]. The most common drug–drug interactions are mainly cytochrome P450 (CYP450)-mediated drug interactions. Five of the P450s (P450 3A4, 3A5,

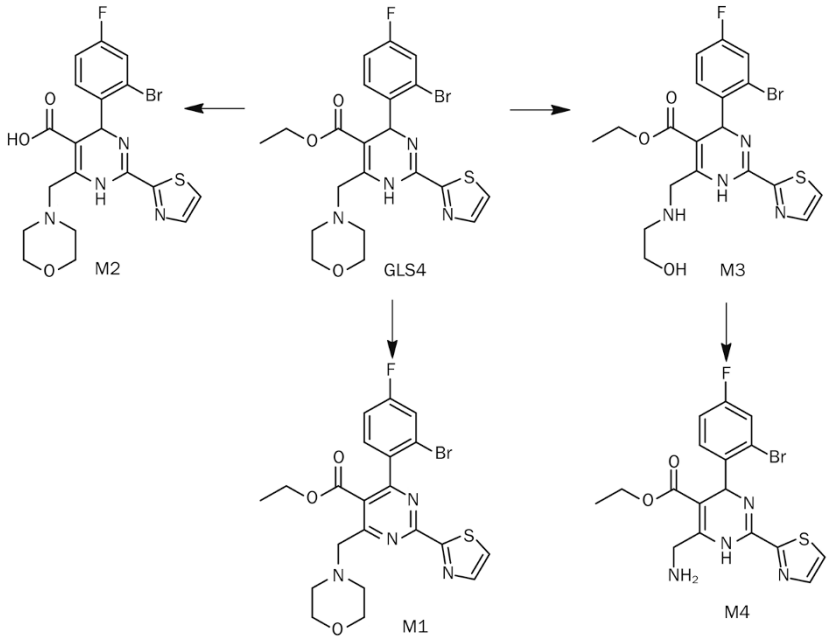

Figure 1. Major metabolic pathways of GLS4 in dog liver microsomes.

2D6, 2C9, and 2C19) account for about 90% of the reactions, and a single CYP3A4 is involved in approximately half of these reactions[10]. Inhibition or induction of CYP3A4 activity is most likely to produce drug–drug interactions. Ketoconazole is a potent inhibitor of CYP3A4 with a K_i value as low as 15 nmol/L[11], whereas rifampicin is reported to be a potent inducer of CYP3A4[12]. Thus, co-administration of ketoconazole or rifampicin with drugs that are known as substrates of CYP3A4 may significantly affect the systemic exposures of co-administered drugs. For example, co-administration of ketoconazole or rifampicin with the sensitive CYP3A substrate midazolam resulted in a 16-fold increase[13] and 98% decrease[14] in the area under the concentration-time curve (AUC) of midazolam, respectively. Both agents have thus been commonly used as prototype drugs for evaluating drug interactions involving CYP3A4 inhibition or induction mechanisms[9, 15].

Preliminary studies of GLS4 in human liver microsomes have indicated that GLS4 is probably a CYP3A substrate. Thus, the objective of the present study is to elucidate whether or not the metabolism and pharmacokinetics of GLS4 are affected by the modulation of CYP3A in dogs. The findings may provide a solid foundation for future studies on clinical drug–drug interactions.

Materials and methods

Chemicals and reagents

GLS4, D_8-GLS4 (internal standard, IS), aromatized GLS4 (M1), ester-hydrolyzed GLS4 (M2), morpholine *N*-dealkylated GLS4 (M3), morpholine *N*,*N*-didealkylated GLS4 (M4), and [^{14}C]GLS4 (specific activity, 40.3 μCi/mg; radiochemical purity, 99.2%) were provided by Hecpharma Co Ltd (Dongguan, China). Ketoconazole was purchased from Damas-beta Co Ltd (Basel, Switzerland), and rifampicin was purchased from Tokyo Kasei Inc (TCI, Tokyo, Japan). Pooled dog and human liver microsomes and recombinant human P450 isoenzyme CYP3A4 were purchased from BD Gentest (Woburn, MA, USA).

Methanol and acetonitrile of HPLC grade were purchased from Sigma (St Louis, MO, USA). Ammonium acetate and formic acid of HPLC grade were purchased from Tedia (Fairfield, OH, USA). HPLC-grade water was obtained from a Millipore Milli-Q gradient water purification system (Molsheim, France).

In vitro incubation with dog and human liver microsomes

Incubation was conducted in duplicate at 37 °C with a total volume of 250 μL. The incubation mixture contained [^{14}C]GLS4 (10 μmol/L) and dog liver microsomes (1.0 mg protein/mL), or human liver microsomes (1.0 mg protein/mL), or CYP3A4 (50 pmol/mL) in 100 mmol/L phosphate buffered solution (pH 7.4). The mixture was pre-incubated for 3 min. The reactions were then initiated by addition of 50 μL NADPH (1 mmol/L) and allowed to proceed for 15 min before termination with ice-cold acetonitrile (250 μL). Inhibition experiments were performed with the CYP3A specific inhibitor ketoconazole (1 μmol/L). The inhibitor was pre-incubated with [^{14}C]GLS4-supplemented dog liver microsomes for 5 min at 37 °C before the reactions were initiated by addition of NADPH. The reactions were quenched as described above.

The metabolites of [^{14}C]GLS4 were detected by gradient HPLC-dynamic online radio flow detection method. HPLC was conducted on an Agilent 1100 HPLC system equipped with a dynamic online radio flow detector (AIM Research

Company, Hockessin, USA). Chromatographic separation was achieved on a XDB C_{18} column (50 mm×4.6 mm ID, 1.8 μm, Agilent, USA). The binary mobile phase consisted of 0.1% formic acid in 5 mmol/L ammonium acetate (A) and acetonitrile (B). The 75-min-long gradient was detailed as follows: 0–2 min, 10% B isocratic, 2–3 min, 10%–25% B linear, 3–30 min, 25%–35% B linear, 30–31 min, 35%–40% B linear, 31–50 min, 40%–100% B linear, 50–60 min, 100% B isocratic, followed by 15 min of re-equilibration of the column before the next run. The flow rate was maintained at 0.6 mL/min, and the injection volume was 90 μL.

Animals

Eight 1-year-old healthy male adult beagle dogs weighing 10–15 kg were used. Each dog was housed in an individual cage and received water *ad libitum* and dry food twice a day (08:00 and 19:00). Protocols for the care and handling of the animals were in accordance with the procedures approved by the Animal Care and Use Committee of Shanghai Institute of Materia Medica (Shanghai, China).

Study design

The beagle dogs were equally divided into Groups A and B. GLS4 was dissolved in 0.5% carboxymethylcellulose sodium. On the first day, all beagle dogs received a single oral gavage dose of 15 mg/kg GLS4. Blood samples (1 mL) were collected from the jugular vein before and 0.5, 1, 1.5, 2, 3, 5, 7, 9, 12, and 24 h post-dosing. Blood samples were placed in heparin-containing tubes and immediately centrifuged at 3000×*g* for 10 min at approximately 4 °C. After a three-day wash-out period, Group A received an oral dose of 100 mg ketoconazole capsule once daily for 8 consecutive days (from d 5 to d 12), whereas Group B received an oral dose of 100 mg rifampicin capsule once daily for 8 consecutive days (from d 5 to d 12). On d 12, all beagle dogs received a single oral gavage dose of 15 mg/kg GLS4 after ketoconazole or rifampicin administration, and blood was sampled up to 24 h as on the first day. All samples were stored at -70 °C until analysis.

Quantitative determination of GLS4 was conducted by HPLC-tandem mass spectrometry (MS/MS) method. The HPLC system utilized a Waters Acquity H-Class System (Waters, USA) and a Waters Acquity FTN autosampler (Waters, USA). Chromatographic separation was performed on an Acquity UPLC BEH C_{18} column (50 mm×2.1 mm, 1.7 μm, Waters, USA). A mixture of acetonitrile-5 mmol/L ammonium acetate-acetic acid (38:62:0.5, *v/v/v*) was used as mobile phase at a flow rate of 0.4 mL/min. The column temperature was maintained at 40 °C.

MS detection was performed on an Acquity Xevo TQ-S system (Waters, USA) in multiple reaction monitoring (MRM) mode. A TurboIonspray ionization (ESI) interface in positive ionization mode was used. Data processing was performed with Masslynx 4.1 software (Waters, USA). The MS/MS parameters were set as follows:

The desolvation gas was set to 1000 L/h at 500 °C, with the source temperature set at 150 °C. The capillary voltage was 3.6 kV. The optimized MRM fragmentation transition for GLS4 was *m/z* 511.1 → *m/z* 220.0 with collision energy of 31 V and cone voltage of 35 V. For D_8-GLS4 (IS), the optimized MRM fragmentation transition was *m/z* 519.1 → *m/z* 108.1 with collision energy of 27 V and cone voltage of 20 V. The scan time was 20 ms.

Plasma GLS4 concentrations were determined after simple protein precipitation. Briefly, the frozen plasma samples were thawed at room temperature and vortexed thoroughly. To a 25 μL aliquot of plasma sample, 10 μL of IS and 100 μL of acetonitrile were added. The mixture was then vortex-mixed for 1 min and then centrifuged at 13 000×*g* for 5 min. A 25 μL aliquot of the supernatant was diluted with 200 μL of the mobile phase, and 10 μL of this mixture was injected into the HPLC-MS/MS system for analysis. The bioanalytical method was validated, and it showed linearity over 1.0–3000 ng/mL with the lower limit of quantification of 1.0 ng/mL.

Pharmacokinetic analysis

The pharmacokinetic parameters of GLS4 were calculated according to a non-compartmental model using WinNonlin (Pharsight Corporation, ver 5.3, Mountain View, CA, USA). The peak concentration (C_{max}), time of peak concentration (T_{max}) and last measurable concentration (C_{last}) were directly obtained by visual inspection of the plasma concentration-time profile. The elimination rate constant (λ) was obtained by the least-squares fitted terminal log-linear portion of the slope of the plasma concentration-time profile. The elimination half-life ($T_{1/2}$) was evaluated according to 0.693/λ. The area under the plasma concentration-time curve from 0 to time t (AUC_{0-t}) was evaluated using the linear trapezoidal rule and further extrapolated to infinity ($AUC_{0-\infty}$) according to the following equation: $AUC_{0-\infty}=AUC_{0-t}+C_{last}/\lambda$. The pharmacokinetic parameters are presented as mean±SEM. Treatment effects were evaluated by Student's *t*-test with $P\leq0.05$ as the level of significance.

Results

In vitro incubation assay

The major metabolic pathways of GLS4 in dog and human liver microsomes are shown in Figure 1. GLS4 underwent extensive metabolism after 15 min incubation in dog and human liver microsomes. Less than 20% of the original amount of GLS4 remained in solution after 15 min incubation. The metabolic profile of [^{14}C]GLS4 in dog liver microsomes (Figure 2A) was similar to that in human liver microsomes and CYP3A4 (Figures 2B and 2C, respectively). The major metabolites were morpholine *N*-dealkylated GLS4 (M3) and morpholine *N*,*N*-di-dealkylated GLS4 (M4). Minor aromatized GLS4 (M1) and ester-hydrolyzed GLS4 (M2) were also detected in dog liver microsomes. All of the metabolic pathways were almost completely inhibited by ketoconazole except ester hydrolysis (Figure 3), which indicated that GLS4 was a sensitive substrate of CYP3A.

Pharmacokinetics of GLS4 affected by ketoconazole

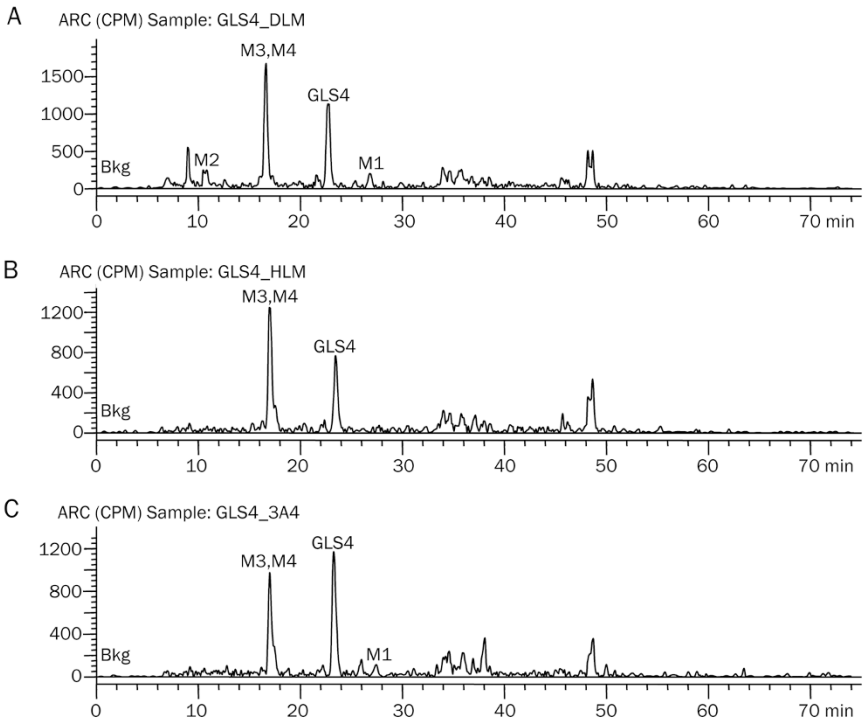

Figure 2. HPLC radioactive chromatograms of [^{14}C]GLS4 after 15 min incubation in (A) dog liver microsomes, (B) human liver microsomes, and (C) CYP3A4.

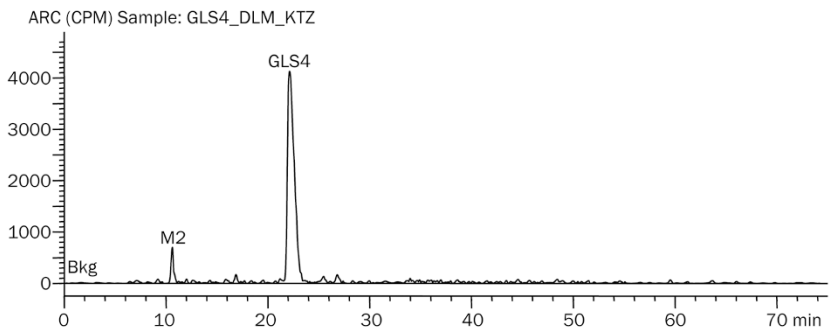

Figure 3. HPLC radioactive chromatogram of [^{14}C]GLS4 after 15-min incubation in dog liver microsomes pretreated with ketoconazole.

The effect of ketoconazole on the pharmacokinetics of GLS4 was investigated by comparing the concentration and kinetic parameters after a single administration of GLS4 with or without ketoconazole pretreatment.

Pretreatment of ketoconazole resulted in a 3.3-fold increase in GLS4 C_{max} (0.445±0.098 μg/mL *vs* 1.38±0.34 μg/mL, P=0.002), 3.9-fold increase in AUC_{0-24} (1.58±0.31 μg·h·mL^{-1} *vs* 5.77±1.46 μg·h·mL^{-1}, P=0.001) and 4.4-fold increase in $AUC_{0-\infty}$ (1.81±0.38 μg·h·mL^{-1} *vs* 7.21±1.72 μg·h·mL^{-1}, P=0.001). Thus, the clearance (*CL/F*) of GLS4 decreased by 75.8% (8.58±1.80 L·h^{-1}·kg^{-1} *vs* 2.18±0.55 L·h^{-1}·kg^{-1}, P=0.001). $T_{1/2}$, T_{max}, and mean residence time (MRT) of GLS4 increased, but no significant changes (P>0.05) were observed after pretreatment with ketoconazole (Table 1, Figure 4).

Pharmacokinetics of GLS4 affected by rifampicin

The effect of rifampicin on the pharmacokinetics of GLS4 was investigated by comparing the concentration and kinetic parameters after a single administration of GLS4 with or without rifampicin as shown in Table 1 and Figure 5.

Pretreatment of rifampicin decreased GLS4 C_{max} by 83.2% (0.481±0.036 μg/mL *vs* 0.0810±0.0127 μg/mL, P<0.01), AUC_{0-24} by 86.8% (1.31±0.09 μg·h·mL^{-1} *vs* 0.173±0.016 μg·h·mL^{-1}, P<0.01), and $AUC_{0-\infty}$ by 88.5% (1.85±0.45 μg·h·mL^{-1} *vs* 0.204±0.012 μg·h·mL^{-1}, P<0.01). Thus, *CL/F* of GLS4 increased by 9.2 folds (8.46±1.88 L·h^{-1}·kg^{-1} *vs* 74.6±4.3 L·h^{-1}·kg^{-1}, P<0.01). $T_{1/2}$ and MRT decreased, but no significant changes were observed (P>0.05) after pretreatment with rifampicin. No

Table 1. Pharmacokinetic parameters of GLS4 after oral administration of 15 mg/kg GLS4 following treatment with 100 mg ketoconazole or 100 mg rifampicin once daily for 8 d.

Treatment		C_{max} (μg/mL)	T_{max} (h)	AUC_{0-t} (μg·h·mL^{-1})	$AUC_{0-\infty}$ (μg·h·mL^{-1})	$T_{1/2}$ (h)	MRT (h)	*CL/F* (L·h^{-1}·kg^{-1})
Group A	GLS4	0.445±0.098	0.875±0.250	1.58±0.31	1.81±0.38	12.1±2.7	5.08±0.69	8.58±1.80
	GLS4+ketoconazole	1.38±0.34	1.12±0.25	5.77±1.46	7.21±1.72	13.3±2.6	6.49±0.22	2.18±0.55
	P-value	0.002	0.207	0.001	0.001	0.554	0.08	0.001
Group B	GLS4	0.481±0.036	0.875±0.250	1.31±0.09	1.85±0.45	16.9±2.5	4.99±0.48	8.46±1.89
	GLS4+rifampicin	0.0810±0.0127	0.875±0.479	0.173±0.016	0.204±0.012	12.9±3.4	4.70±0.65	74.6±4.3
	P-value	<0.001	1.000	<0.001	<0.001	0.106	0.498	<0.001

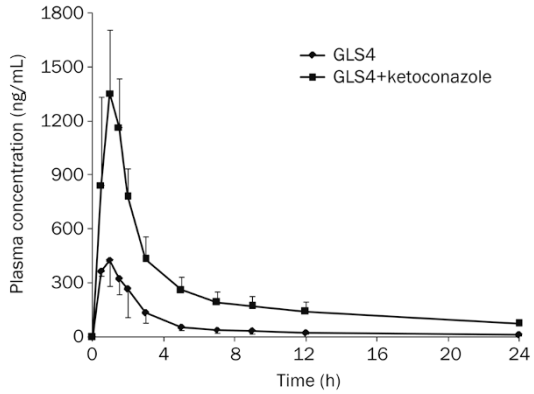

Figure 4. Plasma concentrations of GLS4 in beagle dogs following administration of 15 mg/kg GLS4, before (♦) and after (■) repeated treatment with ketoconazole for 8 d. Mean±SEM.

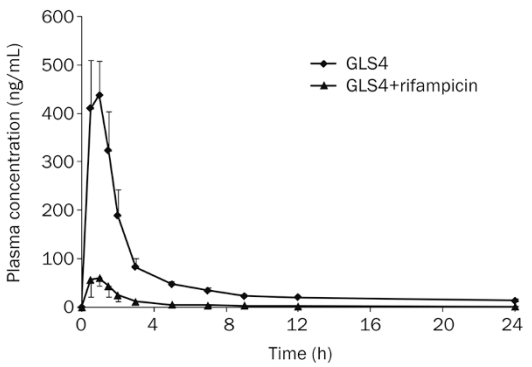

Figure 5. Plasma concentrations of GLS4 in beagle dogs following administration of 15 mg/kg GLS4, before (♦) and after (▲) repeated treatment with rifampicin for 8 d. Mean±SEM.

changes in T_{max} were observed.

Discussion

In vitro incubation with dog and human liver microsomes studies indicated that GLS4 was extensively metabolized. The major metabolic pathway involved was *N*-dealkylation at the morpholine ring, which was mainly catalyzed by CYP3A. *In vivo* studies showed that the plasma concentrations of GLS4 in dogs were significantly affected by pretreatment with ketoconazole (a potent CYP3A inhibitor) and rifampicin (a potent CYP3A inducer). Therefore, the interaction between ketoconazole or rifampicin and GLS4 were most likely resulted from the inhibition or induction of the CYP3A-mediated first-pass metabolism of GLS4.

The beagle dog was selected as an animal model because (1) the metabolic pathways of dogs are much closer to those of humans than those of rats and mice (the major metabolic pathway of GLS4 in rats and mice is ester hydrolysis, and the esterase activities in dogs and humans are considerably lower than those in mice and rats); (2) the plasma concentrations of ketoconazole and rifampicin after oral administration in dogs are also close to those in humans[16, 17]; and (3) the major isozyme of the CYP3A subfamily in canines is CYP3A12, which is parallel to CYP3A4 in humans[18]. Ketoconazole can competitively inhibit CYP3A12 activities[19] and at a therapeutic dose can largely decrease the total body clearance of the CYP3A substrates such as midazolam and nifedipine. Therefore, the beagle dog can be used as an animal model to predict drug–drug interactions between ketoconazole and CYP3A substrates in clinical practice[20]. Kyokawa *et al*[17] reported that the beagle dog can be a suitable animal model for predicting the induction of both hepatic and intestinal CYP3A in humans. Therefore, the effects of ketoconazole and rifampicin on dog CYP3A activities are similar to those on human CYP3A activities, and beagle dogs are appropriate animal models for predicting drug interactions between CYP3A modulators and GLS4.

Ketoconazole and rifampicin affect CYP3A activity both in the liver and gut wall. Co-administration of ketoconazole and rifampicin dramatically affects the pharmacokinetic characteristics of the drugs with high hepatic extraction ratio and intensive CYP3A-mediated first-pass metabolism, such as nifedipine and buspirone[21–23]. In the current study, significant drug–drug interactions between GLS4 and ketoconazole or rifampicin were observed in dogs. Compared with dosing the dogs with GLS4 alone, the concurrent administration of GSL4 with ketoconazole or rifampicin resulted in remarkable changes in the pharmacokinetic parameters of GLS4, including $AUC_{0-\infty}$,

C_{max}, and *CL/F*. All these findings suggested that GLS4 was a sensitive substrate of CYP3A, and first-pass metabolism played an important role in GLS4 elimination.

Although the function of the gut wall in the presystemic metabolism of GLS4 is unknown, the interactions between GLS4 and CYP3A modulators possibly occur in the duodenal wall, as shown by the extensive expression of CYP3A in the duodenal wall[24] and more significant effects on C_{max} and AUC of GLS4 than $T_{1/2}$.

A wide range of CYP3A inhibitors and inducers are typically used in clinical practice. For instance, itraconazole, indinavir, verapamil, and atorvastatin can inhibit CYP3A activity, thereby increase the plasma concentration of the "victim". Safety should be greatly considered when plasma concentration increases. Co-administration of ketoconazole leads to a 35-fold increase in terfenadine plasma exposure, resulting in the heart QT prolongation and torsade de pointes arrhythmia[25]. Terfenadine has been therefore withdrawn from the market, and its metabolite fexofenadine was introduced for clinical use[26, 27]. On the other hand, increased plasma concentration may induce more pharmacological activities. For example, lopinavir/ritonavir is a combination protease inhibitor regimen, in which ritonavir boosts the plasma levels of the active component (lopinavir) by inhibiting its cytochrome P450-mediated metabolism by ritonavir[28]. Aluvia (lopinavir and ritonavir tablets) was introduced in the market for its therapeutic therapy. The "ritonavir boosting" concept may be used for GLS4 if its therapeutic index window is broad enough.

Carbamazepine, phenytoin, and hypericum can induce CYP3A activity. Coadministration of GLS4 with these inducers would lead to the plasma exposure decreases of GLS4, thus affecting its efficacy.

In conclusion, the plasma concentration of GLS4 was significantly affected by pretreatment with ketoconazole or rifampicin, a finding most likely attributable to drug–drug interactions mediated by CYP3A, especially those occurring during first-pass metabolism. The findings strongly suggest that the pharmacokinetics of GLS4 may be affected when it is applied in concomitant therapy with a CYP3A inhibitor or inducer and may yield potentially adverse consequences. Therefore, great attention must be paid to the concomitant administration of a CYP3A modulator with GLS4 in clinical trials to evaluate the effects of treatment.

Acknowledgements

We thank Mr Guo-fang CAI at the Shanghai Institute of Materia Medica (SIMM) for the animal experiments, and Ms Shunbo ZHAO and Wen-juan HU at the SIMM for the determination of GLS4.

Author contribution

Xin ZHOU and Da-fang ZHONG were responsible for the research design, data analysis, and writing of this paper; Zhiwei GAO conducted the animal experiments and pharmacokinetic analysis. Xin ZHOU and Jian MENG were responsible for the analysis of radio-labeled compounds; and Xiao-yan CHEN, a senior advisor, provided valuable advice for this study.

References

1 Institute of Medicine (IOM). Hepatitis and liver cancer: a national strategy for prevention and control of hepatitis B and C. Washington, DC: The National Academies Press; 2010.
2 World Health Organization. Fact Sheet #204: Hepatitis B. 2012 July [cited 2013 Feb 23]. Available from: http://www.who.int/mediacentre/factsheets/fs204/en/ index.html.
3 Loomba R, Liang TJ. Novel approaches to new therapies for hepatitis B virus infection. Antivir Ther 2006; 11: 1–15.
4 Lok AS, McMahon BJ. Chronic hepatitis B. Hepatology 2001; 34: 1225–41.
5 Lai CL, Dienstag J, Schiff E, Leung NW, Atkins M, Hunt C, *et al*. Prevalence and clinical correlates of YMDD variants during lamivudine therapy for patients with chronic hepatitis B. Clin Infect Dis 2003; 36: 687–96.
6 Hadziyannis SJ, Tassopoulos NC, Heathcote EJ, Chang TT, Kitis G, Rizzetto M, *et al*. Long-term therapy with adefovir dipivoxil for HBeAg-negative chronic hepatitis B. N Engl J Med 2005; 352: 2673–81.
7 Deres K, Schröder CH, Paessens A, Goldmann S, Hacker HJ, Weber O, *et al*. Inhibition of hepatitis B virus replication by drug-induced depletion of nucleocapsids. Science 2003; 299: 893–6.
8 Wang XY, Wei ZM, Wu GY, Wang JH, Zhang YJ, Li J, *et al*. *In vitro* inhibition of HBV replication by a novel compound, GLS4, and its efficacy against adefovir-dipivoxil-resistant HBV mutations. Antivir Ther 2012; 17: 793–803.
9 Bjornsson TD, Callaghan JT, Einolf HJ, Fischer V, Gan L, Grimm S, *et al*. The conduct of *in vitro* and *in vivo* drug-drug interaction studies: a pharmaceutical research and manufacturers of America (PhRMA) perspective. Drug Metab Dispos 2003; 31: 815–32.
10 Rendic S. Summary of information on human CYP enzymes: human P450 metabolism data. Drug Metab Rev 2002; 34: 83–448.
11 Achira M, Suzuki H, Ito K, Sugiyama Y. Comparative studies to determine the selective inhibitors for P-glycoprotein and cytochrome P4503A4. AAPS PharmSci 1999; 1: E18.
12 Bolt HM. Rifampicin, a keystone inducer of drug metabolism: from Herbert Remmer's pioneering ideas to modern concepts. Drug Metab Rev 2004; 36: 497–509.
13 Tsunoda SM, Velez RL, von Moltke LL, Greenblatt DJ. Differentiation of intestinal and hepatic cytochrome P450 3A activity with use of midazolam as an *in vivo* probe: effect of ketoconazole. Clin Pharmacol Ther 1999; 66: 461–71.
14 Backman JT, Kivisto KT, Olkkola KT, Neuvonen PJ. The area under the plasma concentration-time curve for oral midazolam is 400-fold larger during treatment with itraconazole than with rifampicin. Eur J Clin Pharmacol 1998; 54: 53–8.
15 FDA, Guidance for industry (draft) drug interaction studies — study design, data analysis, implications for dosing, and labeling recommendations. 2012 Feb [cited 2013 Feb 23]. Available from: http://www.fda.gov/downloads/Drugs/GuidanceComplianceRegulatoryInformation/Guidances/ucm292362.pdf.
16 Baxter JG, Brass C, Schentag JJ, Slaughter RL. Pharmacokinetics of ketoconazole administered intravenously to dogs and orally as tablet and solution to humans and dogs. J Pharm Sci 1986; 75: 443–7.
17 Kyokawa Y, Nishibe Y, Wakabayashi M, Harauchi T, Maruyama T, Baba T, *et al*. Induction of intestinal cytochrome P450 (CYP3A) by rifampicin in beagle dogs. Chem Biol Interact 2001; 134: 291–305.

18 Fraser DJ, Feyereisen R, Harlow GR, Halpert JR. Isolation, heterologous expression and functional characterization of a novel cytochrome P450 3A enzyme from a canine liver cDNA library. J Pharmacol Exp Ther 1997; 283: 1425–32.
19 Kuroha M, Kuze Y, Shimoda M, Kokue E. *In vitro* characterization of the inhibitory effects of ketoconazole on metabolic activities of cytochrome P-450 in canine hepatic microsomes. Am J Vet Res 2002; 63: 900–5.
20 Kuroha M, Shirai Y, Shimoda M. Multiple oral dosing of ketoconazole influences pharmacokinetics of quinidine after intravenous and oral administration in beagle dogs. J Vet Pharmacol Ther 2004; 27: 355–9.
21 Holtbecker N, Fromm MF, Kroemer HK, Ohnhaus EE, Heidemann H. The nifedipine-rifampin interaction. Evidence for induction of gut wall metabolism. Drug Metab Dispos 1996; 24: 1121–3.
22 Kuroha M, Kayaba H, Kishimoto S, Khalil WF, Shimoda M, Kokue E. Effect of oral ketoconazole on first-pass effect of nifedipine after oral administration in dogs. J Pharm Sci 2002; 91: 868–73.
23 Lamberg TS, Kivistö KT, Neuvonen PJ. Concentrations and effects of buspirone are considerably reduced by rifampicin. Br J Clin Pharmacol 1998; 45: 381–5.
24 Kivistö KT, Bookjans G, Fromm MF, Griese EU, Münzel P, Kroemer HK. Expression of CYP3A4, CYP3A5 and CYP3A7 in human duodenal tissue. Br J Clin Pharmacol 1996; 42: 387–9.
25 Boxenbaum H. Cytochrome P450 3A4 *in vivo* ketoconazole competitive inhibition: determination of K_i and dangers associated with high clearance drugs in general. J Pharm Pharm Sci 1999; 2: 47–52.
26 von Moltke LL, Greenblatt DJ, Duan SX, Harmatz JS, Shader RI. *In vitro* prediction of the terfenadine-ketoconazole pharmacokinetic interaction. J Clin Pharmacol 1994; 34: 1222–7.
27 Honig PK, Wortham DC, Zamani K, Conner DP, Mullin JC, Cantilena LR. Terfenadine-ketoconazole interaction. Pharmacokinetic and electrocardiographic consequences. JAMA 1993; 269: 1513–8.
28 Kempf DJ, King MS, Bernstein B, Cernohous P, Bauer E, Moseley J, *et al*. Incidence of resistance in a double-blind study comparing lopinavir/ritonavir plus stavudine and lamivudine to nelfinavir plus stavudine and lamivudine. J Infect Dis 2004; 189: 51–60.